Modeling an Electrostatically Actuated MEMS Diaphragm Pump

by
James Nabity
TDA Research / University of Colorado PhD Candidate
ASEN 5519 Fluid-Structures Interactions
April 2004

Abstract

The recent advent of microelectromechanical systems (MEMS) or micro-devices has generated excitement in many diverse fields. In the area of micro-fluidics liquid pumps are highly desirable for fluid transport and atomization. A recent and popular example of this is the inkjet, which self-aspirates ink from a reservoir and then transports it to a chamber for expulsion as a single droplet during the printing process. Extending this technology to other potential applications requires analytical and computational tools for design. Several computational software packages are commercially available, such as CoventorWare™, FLUENT™, and ANSYS™ [1-3], but each is difficult to use and to date only ANSYS has been able to solve this fully coupled multi-physics problem. Thus, simplified analytical models are attractive for preliminary design and analysis. This paper describes a quasi one-dimensional model developed for the design and analysis of an electrostatically actuated diaphragm pump. The attributes and assumptions of this model will be presented. Finally, performance results obtained for a MEMS diaphragm pump will be compared to ANSYS three-dimensional time-accurate results.

Nomenclature

A	area
d	diameter
E	modulus of elasticity, electric field strength
F	force
g	gravitational constant
G	capacitive gap (also same as fluid gap height)
h	fluid gap height
k_s	spring constant
L	length
$\dot{m}$	mass flow rate
MEMS	microelectromechanical systems or structures
p	gauge pressure relative to ambient
Δp	pressure drop
r	radius
R_h	channel hydraulic radius
t	thickness
u, v	velocity
V	voltage, volume
$\dot{V}$	volumetric flow rate
w	square diaphragm length or width
y	deflection
α	Roarke constant
ε_o	relative permittivity
ε_r	dielectric constant
λ_1	1st eigenvalue from $\lambda_n = \frac{\pi}{a}\left(n - \frac{1}{2}\right)$
μ	viscosity
ν	kinematic viscosity, Poisson's ratio
ρ	density
τ	time constant
subscripts	
e	electrostatic
f	final
$i, 0$	initial
k	spring force
l	liquid
n	eigenvalue equation indice

Station Numbers

1 micropump inlet station
2 micropump nozzle entrance station
e micropump nozzle exit station
∞ ambient

Introduction

The inkjet community has demonstrated a wide variety of devices that incorporate microfluidic flow systems with pumps and valves. Further, this technology has been a great commercial and technological success. Therefore, the question arises as to whether or not this technology can be applied to other industries; specifically, to improve aerospace engine performance.

Several actuation methods have been employed in the inkjet, but we favor electrostatic actuation for its low power. For example the Seiko-Epson electrostatically driven print head [4] shown in Figure 1 applies a low, direct current voltage charge to two parallel plates (the electrode is fixed and the other, a diaphragm pressure plate, is not). Movement of the diaphragm pumps the fluid from a reservoir to the chamber where it is expelled through a nozzle forming a small droplet.

TDA Research and the University of Colorado are currently teamed on three research projects to develop MEMS micropumps for aerospace applications using high voltage electrostatic actuation. In the course of our research we have developed simple analytic models for preliminary design and have applied multi-physics numerical codes to the fully coupled electrostatic-structural-microfluidic micropump problem.

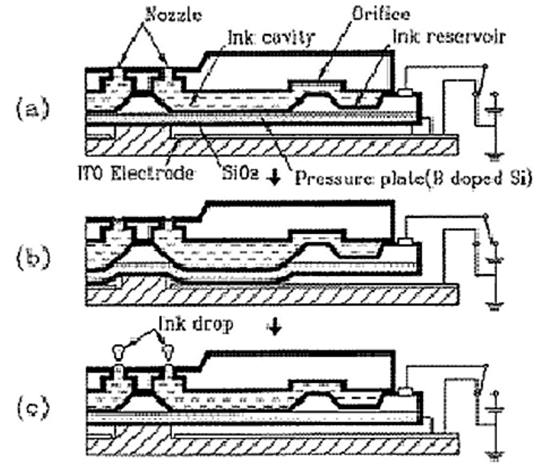

Figure 1. Seiko Epson electrostatic injection: a) initial state, b) DC voltage is applied between pressure plate and electrode, and c) voltage is reduced to zero and droplet is ejected.

Analytical Model Formulation

A one-dimensional model coupling fluidics, electrostatic actuation and the diaphragm structural response was developed to estimate MEMS micropump performance. The problem is one of unsteady flow through a deformable control volume with boundary work acting on the fluid as shown in Figure 2. We assumed that no heat transfer occurs (i.e. adiabatic flow). The sketch also depicts the forces and boundary conditions imposed on the model during the fuel expulsion cycle (details of the fill cycle are not shown). The diaphragm is electrostatically actuated towards the positive or bottom electrode; overcoming the diaphragm spring restoring force and small inertial forces. Assuming a perfect check valve or fluidic diode, the inlet flow is shut-off once the chamber pressure exceeds the fuel delivery pressure. The volumetric flow rate out of the micropump is then equal to the volume displaced by the diaphragm, whose movement depends upon the applied electrostatic force. Also, the entire diaphragm was assumed to move uniformly in the y-direction.

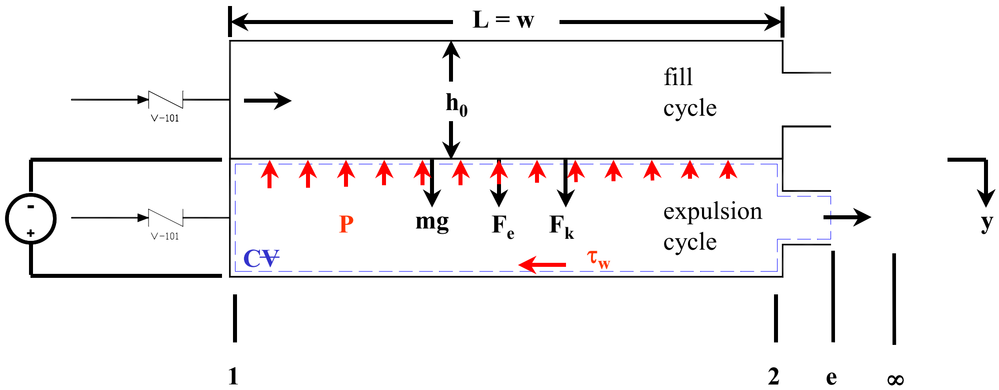

Continuity: $$\dot{m}_e = \rho\vec{\upsilon}(t)A|_e = \rho\vec{\upsilon}(t)A|_1 - \rho\frac{dVol}{dt}$$

x momentum: $$\rho\vec{\upsilon}^2(t)A|_1 + pA|_1 + \rho\frac{d}{dt}\left(\iiint_{CV}\vec{\upsilon}dV\right) - \frac{12\mu\upsilon L}{h}|_f \cdot A_f = \rho\vec{\upsilon}^2(t)A|_2 + pA|_2 = \rho\vec{\upsilon}^2(t)A|_e + pA|_e$$

ΣF of diaphragm: $$\sum F_y = 0 = \vec{F}_e + \vec{F}_k - \vec{p}A + m\vec{g} + \underbrace{\rho\frac{d}{dt}\left(\iiint_{CV}\frac{d\vec{y}}{dt}dV\right)}_{\text{inertial terms} \ll \text{loads at low frequency}}$$

Energy: $$\int \Delta E dm|_{CV} = \int\left(u + \frac{p}{\rho} + \frac{\upsilon^2}{2}\right)dm|_{in} - \int\left(u + \frac{p}{\rho} + \frac{\upsilon^2}{2}\right)dm|_{out} + \int_{y_i}^{y_f}\left(\vec{F}_e + \vec{F}_k\right)dy \quad \text{adiabatic, nonreacting flow}$$

Figure 2. Unsteady, adiabatic, nonreacting and incompressible flow through a deforming control volume.

The diaphragm pumping process is irreversible, since the flow resistance of a Newtonian fluid between closely spaced parallel plates is substantial. If we assume the flow to be quasi-steady, then we may estimate the viscous flow loss between high-aspect ratio parallel plates to be $\Delta P = \frac{12 \cdot \mu \cdot L^* \cdot \upsilon}{h^2}|_{fuel}$ from Hagen-Poiseuille flow, where the diaphragm and positive electrode represent the plates. For circular or 2-d low-aspect ratio flow channels the Hagen-Poiseuille flow pressure loss is given by $\Delta P = \frac{8 \cdot \mu \cdot L \cdot \upsilon}{R_h^2}|_{fuel}$, w/ R_h the hydraulic radius of the channel.

One of the difficulties in model development has been the determination of the correct fluid path length to use for calculating the Poiseuille flow pressure drop. Referring to Figure 3 the path length, L*, must be between 0 and L. The viscous flow length, L^*, will be less than or equal to the length of the diaphragm ($L^* \leq$ w). In fact L^* will approach w/2 if all of the fluid is expelled from the chamber each cycle. However, L^* will be less than w/2, if only some of the chamber is pumped out each cycle. Therefore, L^* was determined from the equivalent fuel displacement volume or $w \cdot L^* \cdot (G_{fuel} - y(t)) = w \cdot L \cdot \Delta y(t)$. Further, the average distance that the fuel travels will actually be ½ of this length, so that $L^* = \frac{1}{2}L \cdot \Delta y(t)/(G_{fuel} - y(t))$.

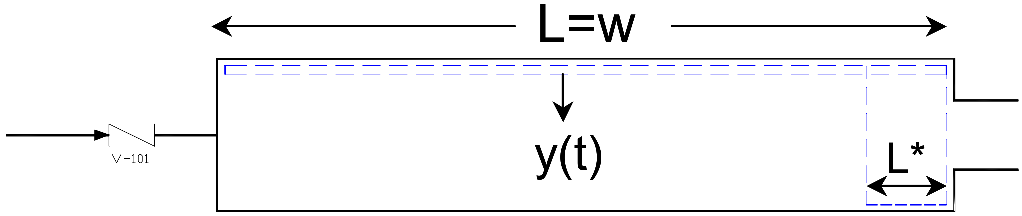

Figure 3. Determination of the fluid path length for Poiseuille flow pressure drop calculation.

Since our flow is transient, these steady flow relations will only provide a good approximation to the actual pressure loss as long as the total expulsion time is large in comparison to the characteristic time of impulsively started flow, which may be approximated by $\tau \approx 1/\nu\lambda_1^2$. Since Daily [5] showed that the impulsively started flow relaxes to the steady state solution within 5-10 τ, the quasi-steady assumption for the micropump will only be valid as long as the expulsion time < 25 τ.

The minimum voltage to electrostatically pull-in or snap-through a diaphragm can be determined from equilibrium of electrostatic and thin plate spring forces (F = qE = k_sy). Thus, the pull-in voltage for a capacitor with two dielectric layers is given by:

$$V_{PI} = \sqrt{\frac{8 \cdot n \cdot k_s \cdot \left(\varepsilon_r \left|_{dielectric} \cdot G_{fuel} + \varepsilon_r \right|_{fuel} \cdot G_{dielectric}\right)^3}{27 \cdot \varepsilon_o \cdot \varepsilon_r \left|_{fuel} \cdot \varepsilon_r^3 \right|_{dielectric} \cdot A}}$$

w $k_s = \dfrac{\pi \cdot K_1^{\;2} \cdot E \cdot t^3}{12 \cdot \left(1-\nu^2\right) \cdot r^2}$ (circular diaphragm)

and $k_s = \dfrac{E \cdot t^3}{\alpha \cdot w^2}$ $w/\alpha = 0.0138$ (square diaphragm)

A summation of forces acting on the diaphragm reveals that the force exerted on the fluid from electrostatic actuation is $\vec{F} = \vec{F}_e + \vec{F}_k$ (self-aspirating pump); the sign(F_e) is always positive, since electrostatics can not generate a repulsive force, and sign(F_k) will depend on the direction of travel of the diaphragm (+ or – y-direction). Therefore, F, is the motive force to expel fluid through the outlet at any time, t.

$$\vec{F}_e(t) = \frac{\tfrac{1}{2}\, \varepsilon_o \varepsilon_r \big|_{fuel} \varepsilon_r^2 \big|_{dielectric} \cdot V^2(t)}{\left[\varepsilon_r \big|_{dielectric} \left(G_{fuel} - \bar{y}(t)\right) + \varepsilon_r \big|_{fuel} G_{dielectric}\right]^2}$$

electrostatic force

ε_o = relative permittivity = 8.85x10^{-6} pF/um
ε_r = dielectric constant ($\varepsilon_r|_{JP\text{-}10}$ = 2.46 and $\varepsilon_r|_{SiO_2}$ = 3.8)
$V(t)$ = actuation voltage
G = gap (either fuel or dielectric)
$y(t)$ = diaphragm displacement

$\vec{F}_k(t) = -k_s \cdot \bar{y}(t)$ diaphragm spring force

Now, the mass or volumetric flow can be determined from Poiseuille flow ($\dot{V}_e = \dot{V}_2 = \dfrac{(p_1 - p_2) \cdot G_f^3}{12 \cdot \mu_f}$), and finally, the diaphragm displacement from continuity ($\bar{y} = \int \left(\dot{V}_e - \dot{V}_1\right) / w^2 \, dt$).

Two assumptions were made in the analysis that can greatly affect micropump performance: first, the use of steady Hagen-Poiseuille flow, and second, the uniform diaphragm displacement a distance y, which closes the fluid gap during fuel expulsion

($G_f = h_0 - y(t)$). We have already discussed the issues associated with the assumption of quasi-steady flow; the expulsion time must be long in comparison to the impulsively started flow transient and the viscous flow length will be about ½ the diaphragm length or less. In the second case, the diaphragm displacement is not uniform as assumed, but rather it is closer to a pyramidal or parabolic profile. Thus, substantial error may be likely for large deflections that approach the fluid gap height.

A set of first-order and algebraic non-linear equations result from the above, which are solved numerically in MathCAD by forward-differencing in time. Mass, momentum and energy are all conserved. Further, only a very small error results in the energy equation, if isothermal flow is assumed.

ANSYS Model Formulation

A 3-dimensional transient CFD analysis of a micropump employing an electrostatically actuated membrane and diffuser-nozzle fluidic diodes has begun (Figure 4). The ANSYS code solves the incompressible Navier Stokes equation. The non-linear pressure velocity coupling is solved using the SIMPLEF scheme. The ALE formulation updates the finite element mesh at each time step according to the applied displacement boundary conditions. The mesh morphing algorithm ensures that the boundary conditions are satisfied. This code simulates the flow field within the device, with the regions of particular interest being the inlet and outlet valves. A weak sequentially coupled analysis is used to model the fluidic-structural interactions. The Arbitrary Lagrangian Eulerian formulation was adopted to solve the fluid flow with moving boundaries. This scheme can accommodate large mesh deformations. Load transfer resulting from the fluidic-structural interaction is allowable across dissimilar meshes along the fluid-solid interface. Simultaneously, a contact analysis simulates the snap down phenomena that induces contact between the common electrode or diaphragm and the positively charged substrate electrode. All structural dof's of the substrate electrode were fixed, whereas the diaphragm was only fixed at the four edges. Three-dimensional surface-to-surface contact elements (TARGE170 and CONTAC173) were generated on the exterior of the model to define the contact surface, which was offset slightly from the diaphragm surface to avoid any singularity within the fluid.

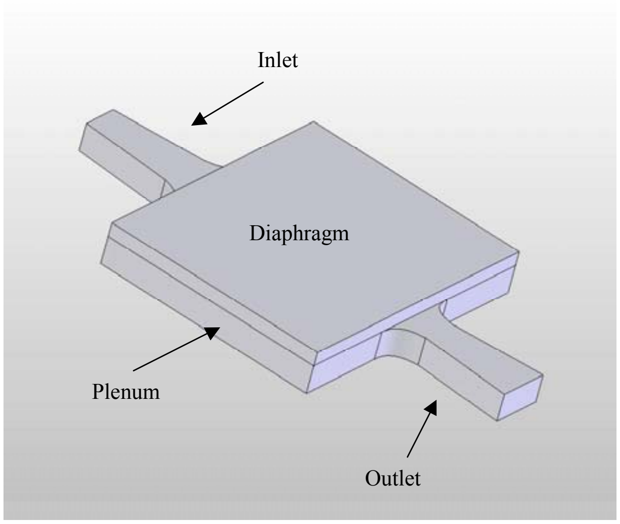

$L_{diaph} = 1000\ \mu m$

$t_{diaph} = 10\ \mu m$

$t_{plenum} = 100\ \mu m$

$t_{passages} = 100\ \mu m$

$L_{passages} = 330\ \mu m$

$W_{inpassages} = 66.7\ \mu m$

$\alpha_{valve} = 5$ degrees

Figure 4. Electrostatically actuated model micropump.

The geometric discretization of the domain was divided into two distinct regions; the fluid (two pump chambers and valves) and the structure (electrodes and diaphragm). An unstructured quadrilateral (FLOTRAN FLUID142 elements) mesh was used to define the fluid regions. The mesh was refined at the inlet valves, outlet nozzle, walls and interface between the diaphragm and fluid, where high gradients were expected. The volumetric mesh was biased towards the walls. The structural region was map meshed using SOLID 54 elements. A plane of symmetry was assumed to reduce the total number of elements needed for a grid independent solution.

Results

The ANSYS model shown in Figure 4 was simulated with a sinusoidal forcing function applied to the diaphragm. The peak displacement was 33um and the frequency was varied from 100 to 1000Hz. Water was used in these simulations. The resulting flow out of the micropump equals the outlet minus the inlet flow (700Hz results shown in Figure 6). This stems from the difference in forward and backward flow resistance characteristic of passive valves. They are designed to have increased flow resistance to back flow, thus ensuring some net positive flow out of the pump.

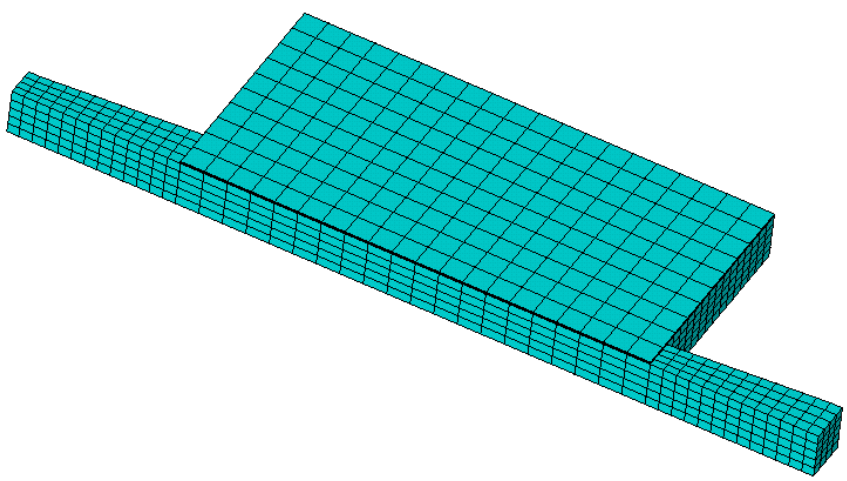

Figure 5. ANSYS meshed model.

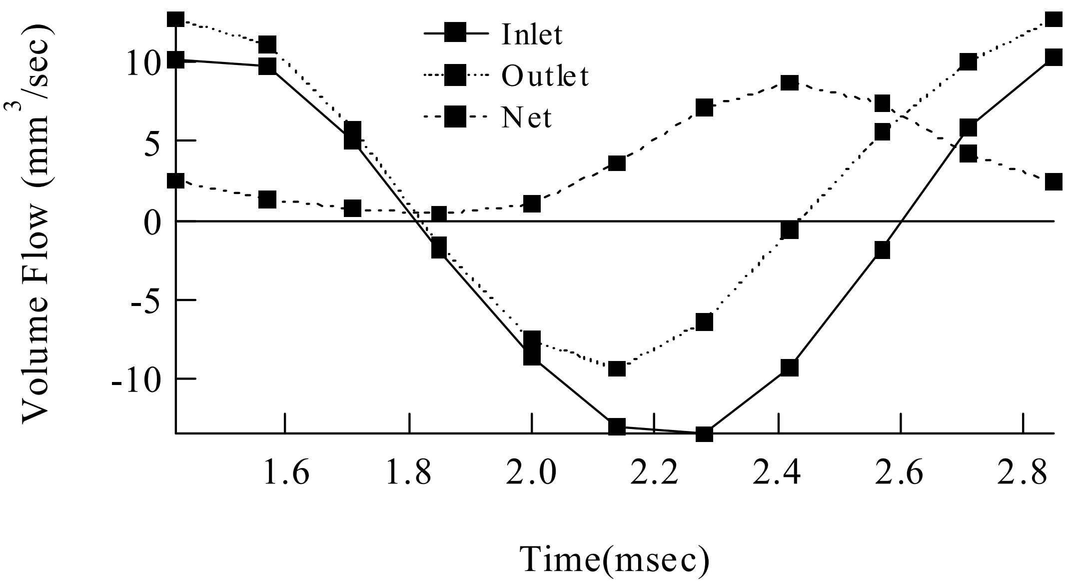

Figure 6. ANSYS predicted micropump flows.

The analytical one-dimensional model was used to simulate the same case and the results were compared to the ANSYS model outputs, which were multiplied by a factor of two to account for the symmetry boundary condition. As seen in Figure 7 a large discrepancy was noted, which was attributed to the assumptions of perfect passive valves and uniform diaphragm displacement in the analytical model. First, the ANSYS flow was adjusted to account for the inefficient passive valves. Second, the analytical model was revised to replace the uniform diaphragm displacement with a pyramidal deflection profile as shown in Figure 8. This reduced the displaced volume by 2/3rds for the same displacement *y(t)*. Good agreement was observed between the models once these changes were implemented (see Figure 9). The discrepancy in flow rate was about 15%.

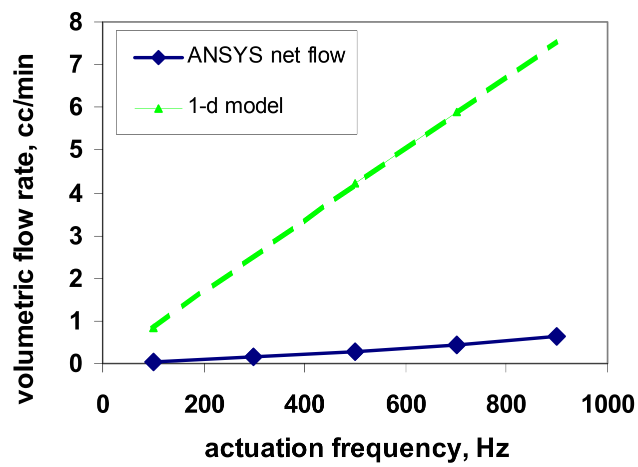

Figure 7. Model comparison of micropump volume flows. 1-d model using uniform diaphragm displacement.

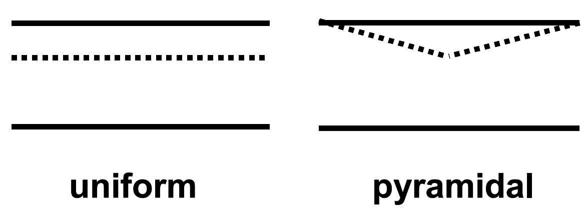

Figure 8. One-dimensional model diaphragm displacement profiles.

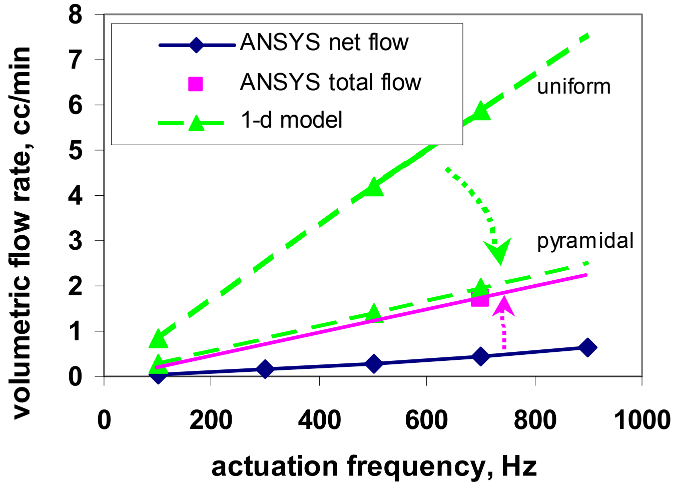

Figure 9. Micropump total flow predictions from ANSYS and one-dimensional models.

Similar results were obtained for the chamber pressure. Again, good agreement was observed between the ANSYS output and the revised analytical model. However, there is a phase shift of about 90 deg, since inertial terms were neglected in the analytical model.

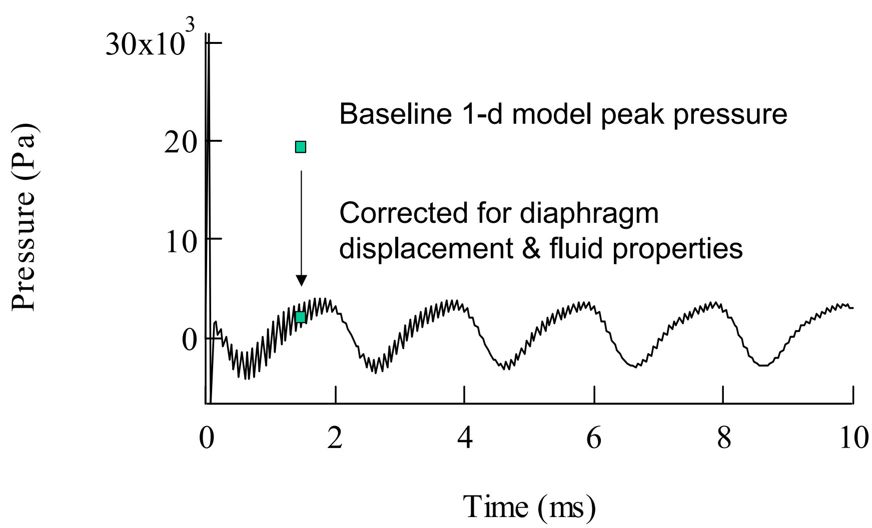

Figure 10. Micropump chamber pressure.

Conclusions

Micropump simulation requires the multiphysics coupling of microfluidics, mechanical interactions and electrostatics. Despite the complex nature of this problem, a simple one-dimensional analytical model was able to predict micropump performance. Thus, a tool has been developed that can be used for parametric evaluation of geometry, fluids, diaphragm materials, and actuation voltage and frequency.

Acknowledgements

This work was sponsored in part by ONR PhII SBIR contract N00014-01-C-0457 'Liquid Fuel Atomizer' monitored by Dr. Chris Brophy, Naval Postgraduate School, Monterey, CA. Also, the ANSYS simulations were conducted with support from the U.S. Air Force Office of Scientific Research (Award no. F49620-02-1-0133). Program Officer Dr. Mitat Birkan, is gratefully acknowledged for his support.

References:

1. ConventorWare™: http://www.coventor.com/coventorware/
2. FLUENT™: http://www.fluent.com/
3. ANSYS™: http://www.ansys.com/
4. S. Kamasuki, M. Fujii, T. Takekoshi, C. Tazuka, and M. Atobe, "A High Resolution, Electrostatically Driven Commercial Inkjet Head," Proceedings of the IEEE Thirteenth Annual International Conference on MEMS, Miyazaki, Japan, 2000.
5. John Daily, "Impulsively Started Channel Flow", personal communication to the author, Nov 2002.